Dual mode acoustic wave sensor for precise pressure reading

Mu, Xiaojing; Kropelnicki, Piotr; Wang, Yong; Randles, Andrew Benson; Chai, Kevin Tshun Chuan; Gu, Yuan Dong; Cai, H.

2014

Mu, X., Kropelnicki, P., Wang, Y., Randles, A. B., Chai, K. T. C., Cai, H.,et al. (2014). Dual mode acoustic wave sensor for precise pressure reading. Applied Physics Letters, 105(11), 113507-.

https://hdl.handle.net/10356/81198

https://doi.org/10.1063/1.4896025

Dual mode acoustic wave sensor for precise pressure reading

Xiaojing Mu, Piotr Kropelnicki, Yong Wang, Andrew Benson Randles, Kevin Tshun Chuan Chai, Hong Cai, and Yuan Dong Gu

Citation: Applied Physics Letters **105**, 113507 (2014); doi: 10.1063/1.4896025
View online: http://dx.doi.org/10.1063/1.4896025
View Table of Contents: http://scitation.aip.org/content/aip/journal/apl/105/11?ver=pdfcov
Published by the AIP Publishing

Dual mode acoustic wave sensor for precise pressure reading

Xiaojing Mu,[1,a)] Piotr Kropelnicki,[1] Yong Wang,[1,2] Andrew Benson Randles,[1] Kevin Tshun Chuan Chai,[1] Hong Cai,[1] and Yuan Dong Gu[1]
[1]*Institute of Microelectronics, Agency for Science, Technology and Research (A*STAR), Singapore 117685*
[2]*The School of Electrical and Electronic Engineering, Nanyang Technology University, Singapore 639798*

(Received 7 August 2014; accepted 3 September 2014; published online 17 September 2014)

In this letter, a Microelectromechanical system acoustic wave sensor, which has a dual mode (lateral field exited Lamb wave mode and surface acoustic wave (SAW) mode) behavior, is presented for precious pressure change read out. Comb-like interdigital structured electrodes on top of piezoelectric material aluminium nitride (AlN) are used to generate the wave modes. The sensor membrane consists of single crystalline silicon formed by backside-etching of the bulk material of a silicon on insulator wafer having variable device thickness layer (5 μm–50 μm). With this principle, a pressure sensor has been fabricated and mounted on a pressure test package with pressure applied to the backside of the membrane within a range of 0 psi to 300 psi. The temperature coefficient of frequency was experimentally measured in the temperature range of −50 °C to 300 °C. This idea demonstrates a piezoelectric based sensor having two modes SAW/Lamb wave for direct physical parameter—pressure readout and temperature cancellation which can operate in harsh environment such as oil and gas exploration, automobile and aeronautic applications using the dual mode behavior of the sensor and differential readout at the same time. © *2014 AIP Publishing LLC*. [http://dx.doi.org/10.1063/1.4896025]

Pressure sensors can be found in several harsh environment application areas, like automotive, aeronautic, or oil-drilling industry.[1–10] Different approaches have been used to sense pressure at higher temperatures. One of these approaches is represented by piezoresistive SiC pressure sensors, which can be used to monitor the pressure of the internal combustion engine with temperatures greater than 300 °C.[11,12] Unfortunately, the accuracy of the piezoresistive sensor decreases when the temperature is higher than 100 °C due to its drop of resistivity.[13] High fabrication costs and up to 300 °C temperature required in harsh environment requirement, creates great demand for new sensor solutions with higher reliability compared to the aforementioned ones.

A promising approach for high temperature operation fell on quartz based resonators, which have been well known as high pressure sensors in harsh environment for a long time.[14,15] A commonly used film bulk acoustic resonator (FBAR) structure has top and bottom electrodes, which help to generate a bulk acoustic wave (BAW) within the quartz material. The pressure information is derived by its resonant frequency read out, which is strongly dependent on stress and temperature of the piezoelectric material. For this reason, a temperature dependent and pressure independent reference sensor is highly needed to calibrate out the temperature effect, which complicates the whole system. Thus three resonators are indispensable for a whole system to extract temperature and pressure separately at the same time.

In this letter, a piezoelectric material AlN based dual mode acoustic wave sensor including surface acoustic wave (SAW) and Lamb wave is developed. This sensor is capable of operating at large temperature ranges from −50 °C to 300 °C and larger pressure ranges from 0 psi to 300 psi. The temperature behaviors of the sensor among these dual modes are almost the same, whereas the pressure sensitivity behaviors are totally different.

With the assistance of a external digital circuit, the temperature effects of the dual mode acoustic wave sensor are likely cancelled out, which results in the sole physical parameter (pressure change) readout.

The fabrication process is Complementary Metal-Oxide-Semiconductor (CMOS) compatible. 8 in. SOI (100) wafers with device layer of 5 μm and 50 μm with buried oxide (BOX) layer of 1 μm were employed. A 100 nm SiO_2 layer was first deposited on the SOI substrate by plasma enhanced chemical vapor deposition (PECVD). After that, a 2 μm AlN piezoelectric layer was deposited by physical vapor deposition (PVD). Then, a 600 nm Al film was grown on AlN and patterned by dry etch to form the Interdigitated Transducer (IDT) structure. A 200 nm SiO_2 was deposited by PECVD and served as hardmask for IDT patterning. After front side process, the silicon substrate layer was thinned down to 400 μm by mechanical grinding. Next, a 2 μm SiO_2 hardmask layer was deposited on the backside of the wafer for release process. Finally the silicon membrane structure was released by deep reactive ion etching (DRIE). Finally, front side SiO_2 is removed by vapor hydrogen fluoride (HF) for contact open. Figure 1 shows the SEM of the IDT electrodes and the cross-sectional structure of the acoustic wave pressure sensor.

Finite element method (FEM) simulations have been carried out by using COMSOL to investigate the performance of the dual mode sensors. 2D simulation was performed using periodic condition on left and right side of the device in order to simulate an infinite, ideal resonator plate. Based on the prior arts,[16,17] the material properties that are used for simulations are summarized in Table I.

[a)]Author to whom correspondence should be addressed. Electronic addresses: mux@ime.a-star.edu.sg and mxjacj@gmail.com

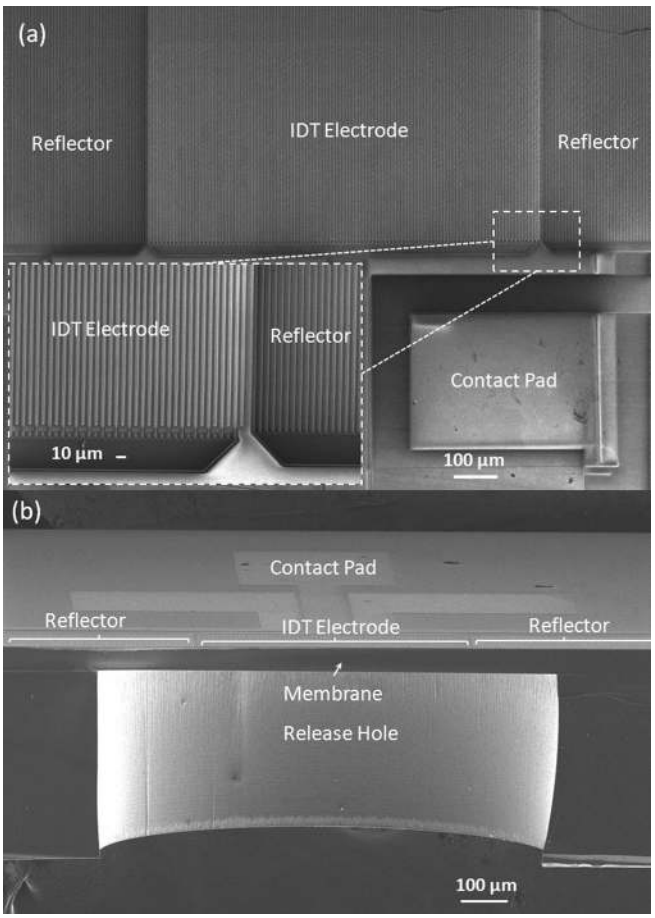

FIG. 1. SEM of (a) top view and (b) the cross-sectional view of the fabricated high temperature acoustic wave pressure sensor.

As observed from Table I, the elastic constants are strongly dependent on temperature, which are almost homogeneously, especially for the first order temperature coefficient. The elastic coefficients are inherently, in the same time, strain/stress dependent.

Based on these assumptions, the resonance frequency of both modes is dependent on the change of the elastic coefficients due to temperature and strain

$$f_s = \frac{v_{ph}}{\lambda}, \quad v_{ph} = \sqrt{\frac{c^*}{p}}, \quad c^* = fct(P,T), \tag{1}$$

where f_s is the resonance frequency, v_{ph} is the phase velocity, λ is the wavelength, p is the density, and c^* is the elastic coefficient of AlN.

According to theory, with thinner membrane, the SAW mode is moving into a S_0 Lamb wave mode as can be seen in Fig. 2. This behavior is normally defined as phase velocity dispersion. Meanwhile, a higher order mode Lamb wave also presents in thick Si membrane devices with strong energy behavior. This higher order Lamb wave exhibits a stable phase velocity throughout a large range of the h (Si)/λ. (Lamb wave high mode as shown in Fig. 2).

From the simulation predictions (as shown in Fig. 2), the SAW mode can be excited at 480.87 MHz when the membrane thickness is larger than one wavelength ($>10\,\mu$m in this case). Most energy of the SAW is concentrated in the depth of one wavelength (λ). Simultaneously, a strong Lamb wave high mode Lamb wave of 973.79 MHz is also observed in this sensor. In this higher order mode, the silicon serves as a transmitting medium, but the energy of the wave is obviously decayed throughout the silicon thickness.

The dual mode pressure sensor with 50 μm thickness silicon membrane is fabricated out for experimental testing. The acoustic wavelength of the device is designed to be 10 μm, which corresponds to an IDT electrode finger width of 2.5 μm. The length and the amount of the IDT electrodes are 1280 μm and 128 pairs, respectively. To serve as pressure sensor, a 1 mm diameter membrane is formed in the center to support the IDT structure. To determine the temperature dependency of resonance frequency of the acoustic wave pressure sensor, high temperature measurements in a range of $-50\,^{\circ}$C to $300\,^{\circ}$C were carried out. By using a Cascade PMV200 vacuum probe station and an Agilent E5071B network analyzer, S-parameters were measured at a series of increasing temperatures. Short-Open-Load-Through (SOLT) method was performed to calibrate the measurand in network analyzer. The chuck of the probe station was heated up with 20 min dwell time before measurement data were collected. In order to reduce the overall measurement noise, an average factor of 10 was selected during the measurement.

Figure 3(a) indicates a second order relationship between resonance frequency and temperature of the SAW mode within a range of $-50\,^{\circ}$C to $300\,^{\circ}$C. As it can be obtained from this figure, the approximated first order and second order temperature coefficient of frequency is extracted to be TCF $= -21.14$ ppm/$^{\circ}$C and TCF2 $= -23.53$ ppb/$^{\circ}$C^2 respectively, which shows comparable behavior with what have been reported in previous literatures.[17] Experimentally, the resonance frequency peak of SAW mode is found at 478 MHz, and this measurement data have a good agreement with FEM simulations (480.87 MHz). At the same time, a higher frequency peak of 988 MHz (Higher order Lamb wave mode) (Fig. 3(b)) is also observed with a strong energy, which shows similar temperature characteristics with the SAW mode due to likewise stiffness coefficients as described before.

With respect to pressure coefficient of frequency (PCF) characterization, pressure was applied on the backside of the membrane in a range of 0 psi to 300 psi using pressurized silicone oil (as shown in Fig. 4(c)). The devices were mounted to an adapter with liquid epoxy and cured at $170\,^{\circ}$C. The adapter was then connected to a pressure controller by a pipe to facilitate coupling the pressurized silicone oil flow to the membrane. Metal wires were bonded to the contact pads on the MEMS device to measure pressure dependent resonance frequency change by the network analyzer.

The relationship between resonance frequency and pressure of the SAW and Lamb wave mode within the range of 0 psi to 300 psi are demonstrated in Figs. 4(a) and 4(b), respectively. Obviously, a positive PCF of $+0.227$ ppm/psi is derived from Fig. 4(a) for SAW mode, while a negative PCF of -0.617 ppm/psi is obtained for Lamb wave mode. This can be explained: like mentioned above, stress induced frequency shift by external applied pressure on different modes is dominated by different elastic constants.

TABLE I. The material used for simulation.

		AlN		Si	SiO_2	Al
Elastic constants, c_{ij} [GPa]	c_{11}	410.06	Young's modulus, E [GPa]	170	70	70
	c_{12}	100.69				
	c_{13}	83.82				
	c_{33}	386.24				
	c_{44}	100.58				
	c_{66}	154.70				
First order temperature coefficient of elastic constants, Tc_{ij} [10^{-6}/K]	Tc_{11}	−10.65	first order temperature coefficient of Young's modulus, TCE [10^{-6}/K]	−63	204	…
	Tc_{12}	−11.67				
	Tc_{13}	−11.22				
	Tc_{33}	−11.13				
	Tc_{44}	−10.82				
	Tc_{66}	−10.80				
Second order temperature coefficient of elastic constants, $T2c_{ij}$ [10^{-9}/K^2]	$T2c_{11}$	−20.61	second order temperature coefficient of Young's modulus, $TCE2$ [10^{-9}/K^2]	−52	221	…
	$T2c_{12}$	−19.51				
	$T2c_{13}$	−19.88				
	$T2c_{33}$	−20.03				
	$T2c_{44}$	−20.36				
	$T2c_{66}$	−20.39				
Piezoelectric stress coefficients, e_{ij} [C/m]	e_{15}	−0.48	…	…	…	…
	e_{31}	−0.58		…	…	
	e_{33}	1.55				
Relative permittivity, ε_{ij}	ε_{11}	9		11.7	4.2	…
	ε_{33}	11		11.7	4.2	…
Thermal expansion, α_{ij} [10^{-6}/K]	α_{11}	5.27		2.6	0.55	18
	α_{33}	4.15		2.6	0.55	18
Mass density, ρ [kg/m^3]		3260		2329	2200	2700

In the previous sections, temperature and pressure sensitivity of our sensor were discussed. Due to the fact that the temperature behavior is almost the same for the both modes while the pressure behavior differs, this behavior leads to possible temperature compensation methods for readout designs. Dual-mode MEMS resonator is driven by external connected oscillator circuits,[18] the two resonant frequencies (f_{Lamb} and f_{SAW}) of which are generated and further quantized into digital signal through the digital counters. Once resonant frequencies are read out, a ratio n can be calculated as

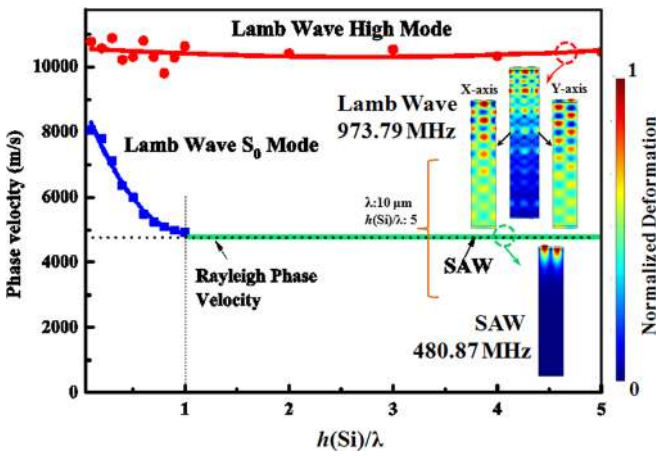

FIG. 2. Simulation on the wave behavior for SAW mode and Lamb wave mode.

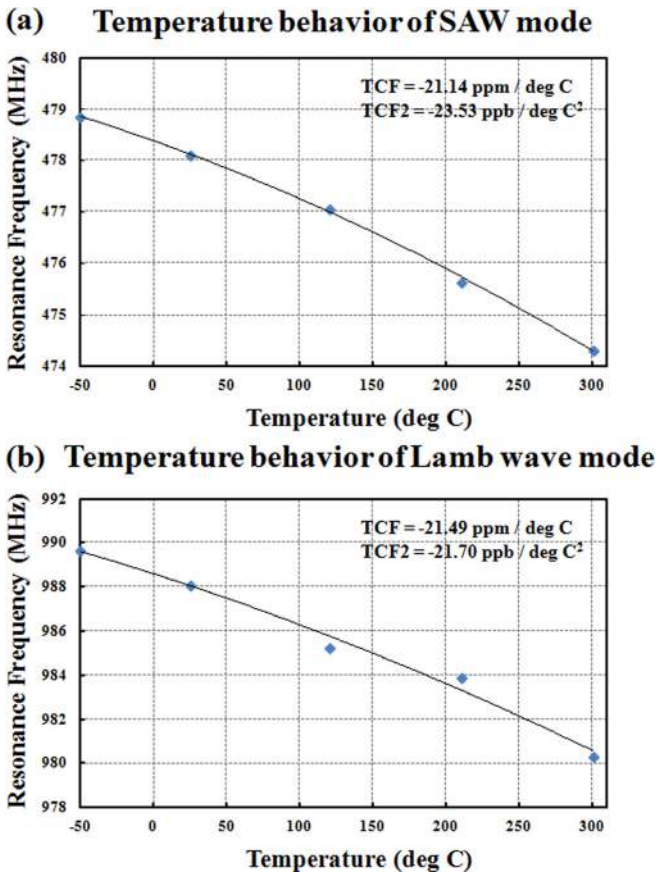

FIG. 3. Measured temperature behavior for: (a) SAW mode; (b) Lamb wave mode.

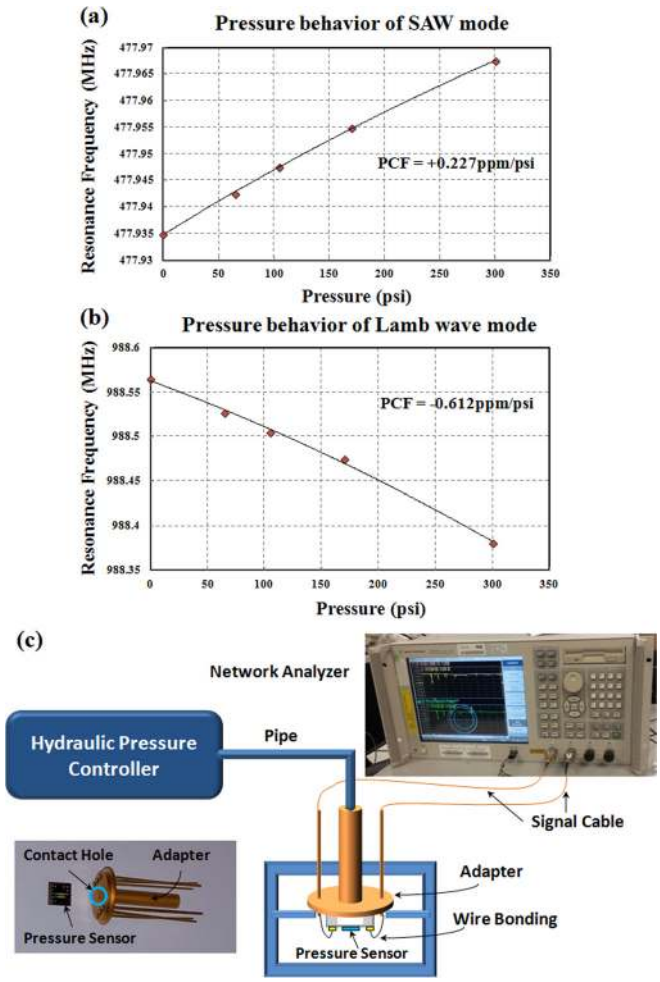

FIG. 4. Measured pressure behavior for: (a) SAW mode; (b) Lamb wave mode; (c) the setup of pressure measurement.

$$n = \frac{f_{Lamb}}{f_{SAW}} \text{ with } n \approx 2.066661,$$

where f_{Lamb} and f_{SAW} are the resonant frequencies of the Lamb mode and SAW mode of the dual mode resonator at 25 °C, respectively. Beat frequency is defines as

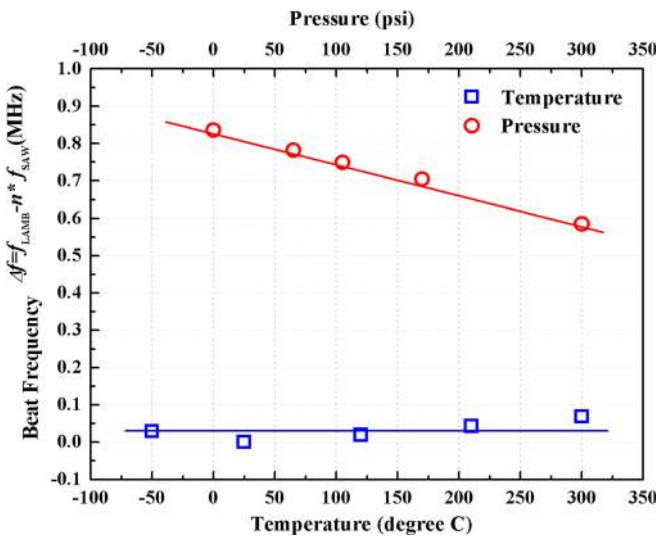

FIG. 5. Relative change of beat frequency for temperature and pressure.

$$\Delta f = f_{Lamb} - n \times f_{SAW}. \quad (2)$$

This frequency can be obtained by feeding the two frequencies into subtractor and multiplier circuits. The f_{SAW} is multiplied by the frequency ratio n and then has a subtraction calculation with f_{Lamb}. Figure 5 depicts that beat frequency Δf varies separately versus temperature and pressure, in range of −50 °C to 300 °C and 0 psi to 300 psi, respectively. As shown in Fig. 5, Δf is approximate constant within the temperature range, implying that it is insensitive to temperature; whereas, the ramp line corresponding to the pressure (ranges from 0 psi to 300 psi) indicates a superior sensitivity. Thus, a precise pressure reading is realized by this dual mode sensor-digital circuit system.

We present prototype of a MEMS dual mode resonator for precise pressure monitoring. Comb-like interdigital electrodes on the top of piezoelectric material-Si stack membrane is employed to generate waves. The waves generated in this sensor mainly have two different modes (SAW and Lamb wave). The TCF of these two modes have been experimentally verified almost the same, while the PCF of them differs. Benefits from dual mode feature, the temperature induced frequency shift is likely suppressed through the logical operation on two readout frequencies by the integrated digital circuit. All in all, more precise pressure readout is realized by utilizing such dual mode resonator-oscillator-digital circuits system.

This work was supported by the Agency for Science, Technology and Research (A*STAR) under Science and Engineering Research Council (SERC) Grant No. 1021650084.

[1]Y. Hezarjaribi, M. N. Hamidon, S. H. Keshmiri, and A. R. Bahadorimehr "Capacitive pressure sensors based on MEMS, operating in harsh environments," *IEEE International Conference on Semiconductor Electronics (ICSE), 25–27 November 2008* (IEEE, Piscataway, NJ, USA, 2008), pp. 184-187.
[2]C. Kolle, W. Scherr, D. Hammerschmidt, G. Pichler, M. Motz, B. Schaffer, B. Forster, and U. Ausserlechner, "Ultra low-power monolithically integrated, capacitive pressure sensor for tire pressure monitoring," in *Proceedings of the IEEE Sensors 2004, 24–27 October 2004* (IEEE, Piscataway, NJ, USA, 2004), pp. 244-247.
[3]Y. Zhang, R. Howver, B. Gogoi, and N. Yazdi, "A high-sensitive ultra-thin MEMS capacitive pressure sensor," In *Transducers 2011–2011 16th International Solid-State Sensors, Actuators and Microsystems Conference, 5–9 June 2011* (IEEE, Piscataway, NJ, USA, 2011), PP. 112–115.
[4]A. M. Anis, M. M. Abutaleb, H. F. Ragai, and M. I. Eladawy, "SiC capacitive pressure sensor node for harsh industrial environment," in 2011 *Third International Conference on Computational Intelligence, Modelling and simulation, 20–22 September 2011* (IEEE Computer Society, Los Alamitos, CA, USA, 2011), PP. 413–416.
[5]L. Lou, S. Zhang, W.-T. Park, J. M.-L. Tsai, D.-L. Kwong, and C. Lee, "Optimization of NEMS pressure sensors with multilayered diaphragm using silicon nanowires as piezoresistive sensing elements," J. Micromech. Microeng. **22**(5), 055012 (2012).
[6]S. Dakshinamurthy, N. R. Quick, and A. Kar, "SiC-based optical interferometry at high pressures and temperatures for pressure and chemical sensing," J. Appl. Phys. **99**, 094902 (2006).
[7]J. Xu, G. Pickrell, X. Wang, W. Peng, K. Cooper, and A. Wang, "A novel temperature-insensitive optical fiber pressure sensor for harsh environments," IEEE Photonics Technol. Lett. **17**(4), 870–872 (2005).
[8]L. S. Pakula, H. Yang, H. T. M. Pham, P. J. French, and P. M. Sarro, "Fabrication of a CMOS compatible pressure sensor for harsh environments," J. Micromech. Microeng. **14**(11), 1478 (2004).
[9]H. San, H. Zhang, Q. Zhang, Y. Yu, and X. Chen, "Silicon-glass-based single piezoresistive pressure sensors for harsh environment applications," J. Micromech. Microeng. **23**(7), 075020 (2013).

[10]X. Zhao, J. M. Tsai, H. Cai, X. M. Ji, J. Zhou, M. H. Bao, Y. P. Huang, D. L. Kwong, and A. Q. Liu, "A nano-opto-mechanical pressure sensor via ring resonator," Opt. Express **20**(8), 8535–8542 (2012).
[11]R. S. Okojie, C. W. Chang, and L. J. Evans, "Reducing DRIE-induced trench effects in SiC pressure sensors using FEA prediction," J. Microelectromech. Syst. **20**, 1174–1183 (2011).
[12]R. S. Okojie, A. A. Ned, and A. D. Kurtz, "Operation of (6H)-SiC pressure sensor at 500 °C," in *Proceedings of International Solid State Sensors and Actuators Conference* (Transducers '97), 16–19 June 1997, (IEEE, New York, NY, USA, 1997), pp. 1407-1409.
[13]A. A. Ned, R. S. Okojie, and A. D. Kurtz, "6H-SiC pressure sensor operation at 600 °C," in *1998 Fourth International High Temperature Electronics Conference*, HITEC, 14–18 June 1998 (IEEE, New York, NY, USA), pp. 257-260.
[14]L. D. Clayton and E. P. EerNisse, "Quartz thickness-shear mode pressure sensor design for enhanced sensitivity," IEEE Trans. Ultrason., Ferroelectr., Freq. Control **45**, 1196–1203 (1998).
[15]R. J. Besson, J. J. Boy, B. Glotin, Y. Jinzaki, B. K. Sinha, and M. Valdois, "A dual-mode thickness-shear quartz pressure sensor," in *IEEE 1991 Ultrasonics Symposium proceedings (Cat. No. 91CH3079-1), 8–11 December 1991*, (IEEE, New York, NY, USA, 1991), pp. 485–493.
[16]D. K. Pandey and R. R. Yadav, "Temperature dependent ultrasonic properties of aluminium nitride," Appl. Acoust. **70**(3), 412–415 (2009).
[17]J. Bjurstrom, G. Wingqvist, V. Yantchev, and I. Katardjiev, "Temperature compensation of liquid FBAR sensors," J. Micromech. Microeng. **17**, 651–658 (2007).
[18]S. S. Schodowski "Resonator self-temperature sensing using a dual-harmonic-mode crystal oscillator," in *43rd Annual Symposium on Frequency Control 1989* (IEEE, 1989).